FORGE WP2
Gas generation state-of-the art and WP2 experiment specifications

FORGE Report D2.1 – VER.1 (February 2012)

	Name	Organisation	Signature	Date
Compiled	D. Stammose A. Vokal	IRSN (France) NRI (Czech Rep.)		23/02/12
Verified	D. Pellegrini	IRSN (France)		23/02/12
Approved	R. Shaw	NERC BGS (UK)		

Keywords

Hydrogen generation, corrosion, carbon steel, bentonite, irradiation.

Bibliographical reference

Stammose, D., Vokal, A.. 2012. Gas generation state-of-the art and WP2 experiment specifications.

FORGE Report D2.1. 37 pp.

Euratom 7th Framework Programme Project: FORGE

EURATOM

Fate of repository gases (FORGE)

The multiple barrier concept is the cornerstone of all proposed schemes for underground disposal of radioactive wastes. The concept invokes a series of barriers, both engineered and natural, between the waste and the surface. Achieving this concept is the primary objective of all disposal programmes, from site appraisal and characterisation to repository design and construction. However, the performance of the repository as a whole (waste, buffer, engineering disturbed zone, host rock), and in particular its gas transport properties, are still poorly understood. Issues still to be adequately examined that relate to understanding basic processes include: dilational versus visco-capillary flow mechanisms; long-term integrity of seals, in particular gas flow along contacts; role of the EDZ as a conduit for preferential flow; laboratory to field up-scaling. Understanding gas generation and migration is thus vital in the quantitative assessment of repositories and is the focus of the research in this integrated, multi-disciplinary project. The FORGE project is a pan-European project with links to international radioactive waste management organisations, regulators and academia, specifically designed to tackle the key research issues associated with the generation and movement of repository gasses. Of particular importance are the long-term performance of bentonite buffers, plastic clays, indurated mudrocks and crystalline formations. Further experimental data are required to reduce uncertainty relating to the quantitative treatment of gas in performance assessment. FORGE will address these issues through a series of laboratory and field-scale experiments, including the development of new methods for up-scaling allowing the optimisation of concepts through detailed scenario analysis. The FORGE partners are committed to training and CPD through a broad portfolio of training opportunities and initiatives which form a significant part of the project.

Further details on the FORGE project and its outcomes can be accessed at www.FORGEproject.org.

Contact details:

EC FORGE Work Package 2 Leader:

Dr Delphine PELLEGRINI
Organisation: IRSN
Tel: 33 (1) 58 35 74 53
Fax 33 (1) 58 35 79 76
email: delphine.pellegrini@irsn.fr
web address: www.irsn.fr
Address: 31 avenue de la Division Leclerc
92260 Fontenay aux Roses Cedex
FRANCE

..

Acknowledgements

Of the many individuals who have contributed to the project, the authors would particularly like to thank the following:

Mr D. DOBREV from NRI (Czech Republic)

Mr. P. BRUHA from NRI (Czech Republic)

Dr L. BERGER from IRSN/PSN-RES/SCA/BIREN (France)

Mr. M. RABOIN from IRSN/PSN-RES/SCA/BIREN (France)

Contents

Acknowledgements ii

Contents iii

Summary v

1 Introduction 1

2 State of the art 1

2.1 Corrosion 1

2.1.1 Corrosion mechanisms of iron and carbon steels 1

2.1.2 Carbon steel corrosion and hydrogen production rates under repository conditions 5

2.1.3 Conclusions 10

2.2 Irradiation 10

2.2.1 Radiolysis of solutions 11

2.2.2 Radiolysis modelling 13

2.2.3 Influence of radiation on corrosion 14

2.2.4 Conclusions 17

3 Experimental program 17

3.1 NRI experiments 17

3.1.1 Equipment for measuring of hydrogen evolution from Carbon steel in anaerobic box 17

3.1.2 Equipment for Measuring of hydrogen migration through compacted bentonite with and without backpressure 18

3.1.3 Equipment for measuring hydrogen evolution rate in contact of carbon steel with bentonite 20

3.1.4 Equipment for measuring hydrogen evolution under irradiation (cooperation with IRSN) 21

3.2 IRSN Experiments 23

3.2.1 Definition of the irradiation conditions 23

3.2.2 Analyses 25

3.2.3 Implementation of input files in Chemsimul for radiolysis simulations 25

3.2.4 Experimental plan 26

4 References 27

Appendix 1: Composition of clay pore waters for 3 different clay dry densities 30

Appendix 2: Example of input file for CHEMSIMUL 31

List of Figures

Figure 1: The change of diffusion coefficient for oxygen with respect to density of bentonite, from Manaka et al. (2000) 4
Figure 2: Effect of pH on hydrogen production 7
Figure 3: Hydrogen production by irradiated water as a function of dose rate 14
Figure 4: Influence of carbonate on hydrogen production – dose rate = 10kGy/h 14
Figure 5: An example of reactions occurring at the interface of carbon steel solution under irradiation (from Zhang et al., 2007). 15
Figure 6: Equipment for measuring hydrogen evolution in anaerobic box 17
Figure 7: Scheme of device for measuring hydrogen migration without backpressure 19
Figure 8: Scheme of device for measuring hydrogen migration with backpressure from compression machine 19
Figure 9: Sample of saturated bentonite Rokle for measuring hydrogen migration 20
Figure 10: Corrosion chamber for measuring hydrogen evolution from carbon steel in contact with compacted bentonite 21
Figure 11: The corrosion chamber for measuring hydrogen evolution under radiation before modification 22
Figure 12: Picture of corrosion cell after irradiation by Co-60 22
Figure 13 : IRMA facility 24
Figure 14: Representation of the structure of the cell 25

List of Tables

Table 1: Hydrogen formation rates at various conditions (Jelinek and Neufeld, 1982, Gould and Evans, 1947) 5
Table 2: Hydrogen production from corrosion of iron in real granitic water (Simpson et al., 1985) 6
Table 3: Yields (number of molecules produced or consumed per 100 eV of adsorbed energy) of primary species (Pastina, 1997) 11
Table 4: Composition of bentonite synthetic water 18
Table 5: Composition of carbon steel 18
Table 6: Characteristics of ^{60}Co sources 24

Summary

This first report produced within Work Package 2 of the European project FORGE intends to gather knowledge available at the start of the project regarding hydrogen generation from corrosion of iron and carbon steel components. It also aims at giving the main specification outlines of the experiment planned within WP2 (as seen after the first 1-year period of the FORGE project), so as to set the surroundings for further advancement of WP2 work.

The state-of-the-art drawn at the onset of the project shows that very high hydrogen generation rates (about 20 $mol.m^{-2}.yr^{-1}$) can be reached at the beginning of corrosion until a corrosion layer is formed on the metal surface. After some time corrosion rate will decrease to much lower values, certainly below 5 μm/yr, which corresponds to hydrogen generation rates lower than 1 $mol.m^{-2}.yr^{-1}$. However this review confirms that, despite the work already done to study iron and carbon steel corrosion mechanisms under various conditions, uncertainties still remain concerning in particular, the effect of content in oxygen, temperature, and chemistry of water and/or solids in presence on corrosion and thus on hydrogen production rates. Besides, there are very little results available on the impact of radiation on corrosion in anaerobic conditions and on hydrogen production/consumption. Current knowledge tends to indicate that the corrosion of carbon steel is enhanced under irradiation, but the processes as well as the quantification are still uncertain.

Thus, an accurate assessment of the evolution of the hydrogen generation rate within a repository due to corrosion of carbon steel components - i.e. the intensity and duration of the "transient" and "steady state" of hydrogen production rate - should rely on a better understanding of the underlying mechanisms for various sets of key parameters representative of repository environments. In this respect, the investigation of the corrosion layers formation, nature and stability appears to be a decisive step.

Several experiments are planned by the two WP2 partners so as to address these key parameters. NRI devices for hydrogen production or hydrogen migration measurements are adapted from equipments used before within the European project NF-PRO; these equipments have been further developed/modified, notably to enable hydrogen evolution measurements for carbon steel in contact with compacted bentonite or under irradiation. Measurements will involve iron or carbon steel samples of various reactive surface (powder, plates, tube), in bentonite synthetic water or in contact with compacted bentonites (Voltex, Rokle), in anaerobic conditions and for various temperatures (up to 70°C). IRSN experiments using the irradiation facility "IRMA" have required numerous tests for the validation of the experimental devices with the strong constraints of i) online gas measurement by gas chromatography and ii) irradiation conditions. Besides the dose calculations performed for the definition of the irradiation conditions, some difficulties have been encountered so that this report mainly focus on the outlines of IRSN objectives in terms of plan of experimental works.

1 Introduction

In the framework of the safety assessment of a geological disposal, one of the issues of concern is the impact of gases produced within the facility, notably in terms of possible perturbations (modification of the water saturation process, fracturing of the host-rock or of engineered components, opening of interfaces…) which may decrease the containment capability of the disposal system. The integrated, multi-disciplinary FORGE project addresses this key research area so as to provide new insights into the processes and mechanisms governing gas generation and migration.

The generation of gases is the object of a specific work package (WP2) within the FORGE project. The main source of gas in a geological disposal of HLW is generally the formation of hydrogen by corrosion of ferrous materials (although it may depend on waste types and disposal design). An accurate assessment of kinetics of hydrogen production/consumption close to the point of origin and of its migration is an important input in the understanding of the likelihood of the development of a discrete phase and of the global evolution of hydrogen within the repository. Thus, WP2 has been focused on the hydrogen source term from corrosion of carbon steel components such as mechanical supports or overpacks. The main expected outcome is to decrease the uncertainties on the effects of parameters representative of repository conditions (T, Eh, reactive surface, solid and/or liquid phases in contact with steel, radiation…), on corrosion rates and consequently on hydrogen production rates. For this purpose, WP2 partners (NRI and IRSN) will carry out experiments under various conditions, which address specific issues related to corrosion and migration (NRI) and corrosion under irradiation (IRSN).

This FORGE Deliverable presents a primary bibliographic review (chapter 2), so as to highlight, with a gas generation perspective, the state-of-the-art at the beginning of the FORGE project regarding iron and carbon steel corrosion under repository conditions, including a specific focus on radiation. It may be worth completing this review, which will serve for interpretation of experimental results, all along the FORGE project. The experiments planned by NRI and IRSN are then documented (chapter 3). A summarised description is given for the four types of equipment as well as the main experimental conditions developed by NRI to assess i) hydrogen generation from carbon steel corrosion in controlled anaerobic and temperature conditions, ii) hydrogen migration through compacted bentonite with and without backpressure, iii) hydrogen generation from carbon steel in contact with bentonite and iv) hydrogen generation under irradiation. A first version of possible specifications of IRSN experimental conditions for assessing radiation impact is then given.

2 State of the art

2.1 CORROSION

2.1.1 Corrosion mechanisms of iron and carbon steels

The corrosion mechanisms of iron and carbon steel depend primarily on physico-chemical conditions, notably the content of oxygen and water in contact with these components. From

this point, deep geological repository (DGR) evolution phases can be divided as follows (derived from Marsh and Taylor, 1988):

- **Aerobic phase** - during the operation phase of a disposal cell and possibly some time after its closure, the overall aerobic corrosion reactions will occur in the unlimited presence of oxygen trapped in the buffer and backfill materials with sufficient flux of oxygen from unsaturated environment (~8 ppm of O_2). No hydrogen is supposed to be generated in this first phase.
- **Limited flux of oxygen** (0.03 – 8 ppm of O_2) – during this phase, the iron/carbon steel environment (buffer, host-rock...) is assumed to be saturated with groundwater (possibly modified by lixiviation of various components, e.g. concrete), so that the mass transport of oxygen to and from the iron/carbon steel surface is by diffusion through water-filled pores. Hydrogen can be generated depending on the content in oxygen.
- **Anaerobic phase** - after consumption of oxygen (< 0.03 ppm of O_2), the groundwater (possibly modified by the alteration of surrounding components) controls the iron/carbon steel environment. Corrosion yields to hydrogen generation, as detailed hereafter.

The time scales of each of these different phases depend on the host rock environment and the design of the repository.

2.1.1.1 AEROBIC PHASE

Corrosion of canisters starts immediately after their manufacture in the atmosphere of storage facilities. The processes of corrosion will depend primarily on the humidity of the air in storage facilities. Dry oxidation phase leads to the steady build up of an oxide layer. In general, the thicker is the oxide layer, the slower is the subsequent oxidation rate. The structure and composition of oxide layer depend on the content of air contaminants, mainly sulphur and nitrogen oxides content.

After achieving a so-called “critical relative humidity” (CRH), a continuous film of water can be formed on metal and corrosion goes in aqueous phase, 10 to 100 times higher than corrosion in "dry" phase (low relative humidity) Achieving of CRH depends on the type of metal and other conditions (Gdowski and Estill, 1996).

The corrosion of iron in pure water under aerobic conditions can be expressed by the following equation:

$$4\,Fe + 2\,H_2O + 3\,O_2 \rightarrow 4\,FeO(OH) \rightarrow 2Fe_2O_3 + 2H_2O \qquad (1)$$

No hydrogen is expected to form under this phase. From thermodynamic point of view the driving force (Gibbs energy = -1374 kJ/mol) of this reaction is very favourable and the reaction is thus practically irreversible. The solubility of formed iron-oxyhydroxides and iron oxides is very low and if no constant removing of solid products would proceed, the general corrosion rate would very quickly slow down due to corrosion products solubilities.

Under some conditions, primarily a high redox potential difference, very adherent and covering solids may be formed on the surface of iron, especially in the alkaline environment. These solid products will passivate the metal and the corrosion will practically decrease to negligible values. The presence of carbonates can contribute significantly to the formation of passive layers on the surface of iron. But this passive film can be breached resulting in localized forms of

degradation, such as pitting, crevice corrosion, stress-corrosion cracking (SCC), or hydrogen embrittlement (HE). In these situations, the rate of localized corrosion is of many orders of magnitude higher than the rate of general corrosion. The tendency of iron to passivation depends primarily on the iron additives. Passivation layers are formed very quickly if the content of Cr is higher than 12 %. Elements like Mo or Ni contribute also to the formation of passivation layers, on the contrary to anions in solution like Cl^- or SO_4^{2-} which disturbe the passive layers.

It is supposed that only under the presence of oxygen, a sufficiently high potential might be generated leading to the passivation of carbon steel surface and possible localized corrosion. The current approaches (Dunn et al., 2000, Druyts et al., 2001) for evaluating the tendency of iron and iron alloys (stainless steels) to localized corrosion are based on determining characteristic potentials of polarisation curves. Values of critical potential for pit nucleation (E_{np}) and critical potential for repassivation (E_{pp}) (protection potential) are compared with the values of corrosion (open circuit) potential (E_{corr}). If E_{corr} exceeds $E_{np,}$ pits will initiate and grow.

If E_{corr} is between E_{np} and E_{pp} existing pits will grow but no new ones will be formed and mechanical damages to a passive layer will give rise to localised corrosion and occurring crevice corrosion will also continue. For E_{corr} below E_{pp} all pits will repassivate.

2.1.1.2 AQUEOUS CORROSION WITH LIMITED FLUX OF OXYGEN

After emplacement of the canisters in DGR, and after sealing all the paths to atmosphere, the host-rock and bentonite will gradually saturate with water and the concentration of trapped oxygen will be reduced by corrosion and microbial reactions. The three following sources of oxygen can be considered in the repository after its closure (Marsh et al., 1987):

- The air trapped in the pore space of buffer and backfill material
- Dissolved oxygen in the groundwater permeating the repository
- Oxygen formed by radiation

It was reported (Marsh et al., 1987) that this period is indefinite if the diffusion coefficient of oxygen in bentonite is 1.2×10^{-10} m^2 s^{-1} and about 130 years if the diffusion coefficient is 1.2×10^{-11} m^2 s^{-1}. The authors, however, assume - very conservatively - that the concentration of oxygen at the floor of repository tunnels remains very high (8 ppm) and constant. This condition is however, as was shown in recent REX project (Puigdomenech et al., 2000, 2001), unrealistic high mainly due to microbial consumption of oxygen during its way to deep groundwater.

In a water saturated bentonite environment, diffusion coefficient of oxygen is decreasing with increasing bentonite density according to Manaka, 2000 (Fig. 1) and therefore the effect of oxygen reactions will quickly decrease.

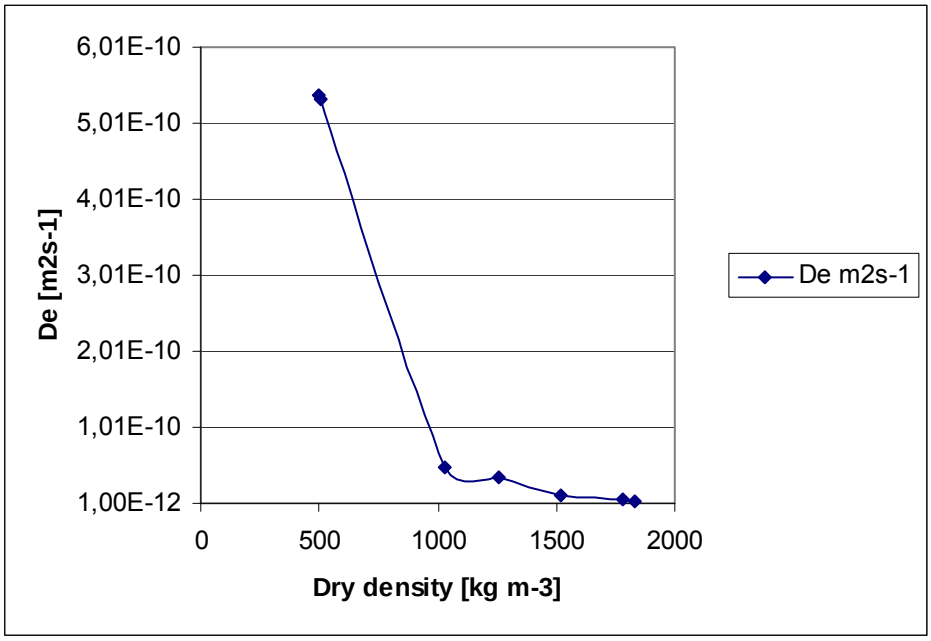

Figure 1: The change of diffusion coefficient for oxygen with respect to density of bentonite, from Manaka et al. (2000)

It seems that in the environment without oxygen, corrosion potential E_{corr} is very low and therefore it not very probable that some type of localized corrosion could be important, but it can be supposed that with a very low concentration of oxygen the passive film cannot be reproduced sufficiently and therefore the corrosion rate becomes higher.

It is expected that during this phase hydrogen can be generated by reactions described below.

2.1.1.3 AQUEOUS ANAEROBIC CORROSION

After some time depending on a number of factors driving oxygen removal in surrounding environment, iron will corrode without any oxygen through the following reaction.

$$\mathbf{Fe(s) + 2H_2O \leftrightarrow Fe(OH)_2(s) + H_2(aq)} \qquad \mathbf{(2)}$$

Ferrous hydroxide is not stable and can easily decompose by so-called Schikorr reaction to magnetite leading again to the formation of hydrogen.

$$\mathbf{3Fe(OH)_2(s) \leftrightarrow Fe_3O_4(s) + 4H_2(aq) + 2H_2O} \qquad \mathbf{(3)}$$

Above 85 ^{o}C iron hydroxide is decomposed through the following reaction without hydrogen generation

$$\mathbf{4Fe(OH)_2(s) \rightarrow Fe_3O_4(s) + Fe(cr) + 4H_2O} \qquad \mathbf{(4)}$$

The Schikkor reaction is very slow under temperatures of about 60 ^{o}C.

Reaction (3) is very often used for computing hydrogen production rate from measuring corrosion rate by weight loss measurement. The following equation was used for recalculation of corrosion rate on hydrogen production rate

$$v_{H_2} = S \times R \times \rho \times m \times \frac{1}{M_{Fe}/1000}$$

where v_{H2} is hydrogen generation rate mol/year, S is reactive surface area (m^2), R is corrosion rate (m/year), ρ is density of iron, m is stoichiometric factor (4/3) for the generation of magnetite (equation (3)) and M_{Fe} is molecular weight of iron (55.85 g/mol).

(In some older publications the results of hydrogen production rate were given in ml m^{-2} d^{-1}. The rate in units of mol m^{-2} yr^{-1} can be obtained by dividing the value by number 61.41).

2.1.2 Carbon steel corrosion and hydrogen production rates under repository conditions

A number of experiments have been devoted to the measurements of carbon steel corrosion and hydrogen production rates (Jelinek, Neufeld, 1982, Simpson, 1984, Simpson et al., 1985, Anantamula et al. 1987, Marsh, Taylor, 1988, Schenk, 1988, Grauer et al., 1991, Hara et al., 1992, Honda et al., 1991, Kozaki et al., 1994, Fujisawa et al.1997, Xia et al., 2005, Smart et al., 2001, 2008) and reviews (Platts et al., 1994, Wiborgh et al., 1986) under simulated repository conditions.

The main outlines are summarized below, for corrosion in solution in a first part and for iron/steel in contact with geomaterials in a second part.

2.1.2.1 Corrosion in solution

Jelinek and Neufeld (1982) measured the hydrogen rate from carbon steel corrosion in pure water or in 0.1 N $NaHCO_3$ solution using gas chromatography methods in the temperature range between 60 and 100° C. The cell with samples was evacuated on a rotary pump and then deaerated water was transferred form to the cell. No content of oxygen in the water is reported in the paper. Various amount of copper was also added to the solution as a potential catalyst of the reactions leading to the hydrogen formation. The results of their measurements are given in the following Table 1.

Table 1: Hydrogen formation rates at various conditions (Jelinek and Neufeld, 1982, Gould and Evans, 1947)

Solution composition	Hydrogen production rate (mol m^{-2} yr^{-1})			
	60°C	80°C	90°C	100°C
Distilled water	0.18	0.2	0.15	0.29
Dist. Water + 0.2 ppm Cu		0.31		
Dist. Water + 1 ppm Cu	0.38	0.20	0.07	
Dist. Water + 10 ppm Cu	0.34	0.33	0.12	
0.1 N $NaHCO_3$	0.14	0.59	0.07	
0.1 N $NaHCO_3$ + 10 ppm Cu	0.07		0.1	
0.05 N $KClO_3$	0.28			

The volumetric hydrogen rate was correlated to weight loss of steel, but not all hydrogen expected from stoichiometric considerations appeared as free gas. Therefore, the corrosion rates predicted using hydrogen production rate are lower (0.8 μm/yr) than those obtained by weight loss measurements (1.3 μm/yr).

The authors found that the average rate of hydrogen production at temperatures below 100°C in distilled water was about 0.16 (mol m^{-2} yr^{-1}). The value of 0.29 (mol m^{-2} yr^{-1}) obtained at 100 °C given in the Table 1 comes from an older publication of Gould and Evans (1947). The hydrogen formation rates were high initially (first days), but slowed down and become linear after approximately 1 week at all three temperatures. The results achieved at 60 °C were relatively least and at 90 °C relatively the most reproducible. A subjective observation indicated the presence of two types of layers on the surface of steel: a top layer, loose and easy to scrape and an inner, more adherent layer.

They did not find any significant temperature dependence in the range 60 to 90°C under the measurement conditions and no catalytic effect of copper.

Simpson (1985), Simpson et al. (1985) and Schenk (1988) measured hydrogen production in real granitic waters (reducing environment) from Säckingen and Böttstein sites and in sodium chloride solutions at temperatures 25, 50 and 80°C and various pH (without oxygen). They used similar chromatographic method for hydrogen quantification as Jelinek and Neufeld (1982). The initial values for hydrogen production from real granitic waters achieved very high values about 27.36 (mol m^{-2} yr^{-1}), but after a short time these high values decreased to values given in Table 2.

Table 2: Hydrogen production from corrosion of iron in real granitic water (Simpson et al., 1985)

Type of granitic water	Hydrogen production rate (mol m^{-2} yr^{-1})		
	25 °C	50 °C	80 °C
Böttstein	0.18	0.98	0.37
Säckingen	0.25	0.51	0.23

The results of hydrogen production rate measured by Simpson et al. (1985) with respect to pH are plotted in Fig. 2 for various chloride concentrations and two temperatures 50 and 80°C.

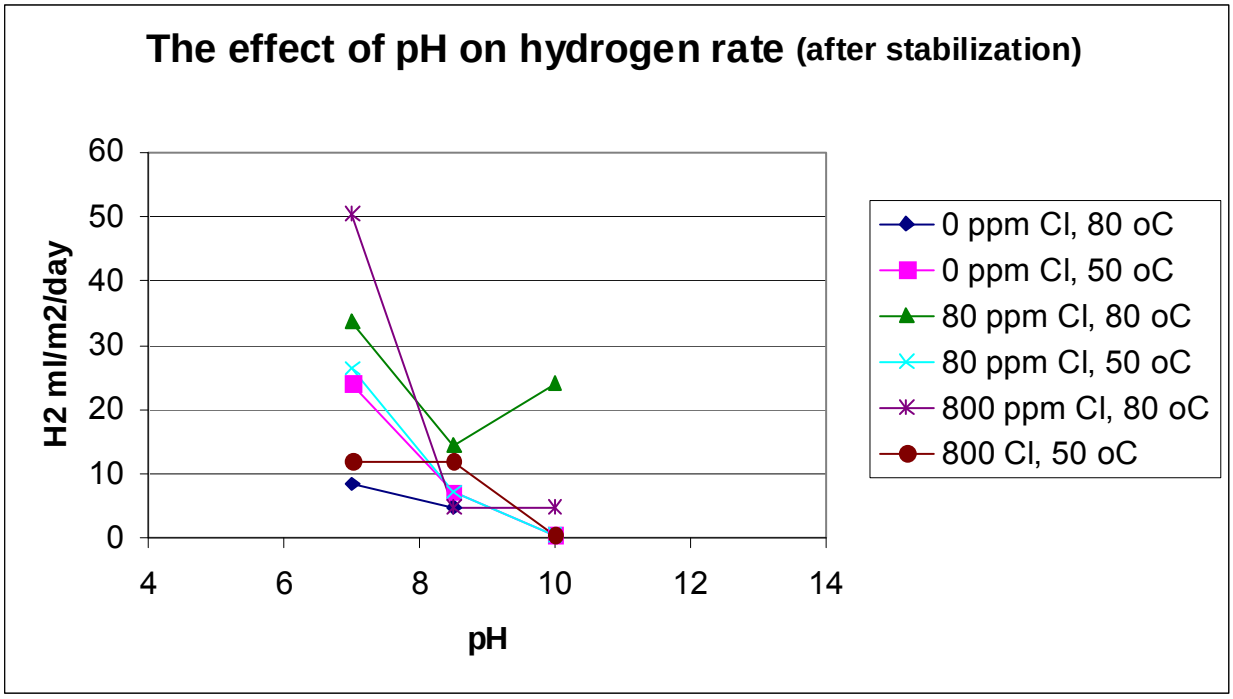

Figure 2: Effect of pH on hydrogen production

It follows from this figure that hydrogen production depends significantly on pH. The effect of temperature does not seem to be significant. The effect of chloride ions concentration is negligible within the range studied. From a comparison of the data in tables 1 and 2 can be derived that the hydrogen production rate of carbon steels in granitic water could achieve more than five times larger values than in distilled water.

For the same groundwaters from the Böttstein site, Grauer et al. (1991) measured hydrogen production rate form iron and steel at 25°C using equipment based on the measurements of volume change. They observed a lower initial rate of hydrogen (0.07 mol m^{-2} yr^{-1}) than Simpson et al. (1984, 1985) and Schenk (1988). This value further decreased to a steady-state value of about 0.005 mol m^{-2} yr^{-1} after more than 8000 hours.

At about pH 10, carbon steels evidently passivate and hydrogen production is negligible. Similar results on the passivity of carbon steel at higher pH were observed also in the papers of Matsuda et al. (1995) or Fujiwara et al. (2001).

Hara et al. (1992) measured hydrogen production rate from carbon steel under various concentrations of oxygen. They found that the volume of hydrogen gas produced tends to increase with increasing dissolved oxygen concentration and this tendency was more noticeable after 30 days immersion of specimens than after 14 days of immersion. The average hydrogen production was about 0.54 $molm^{-2}yr^{-1}$ at the concentration of oxygen of 0.01 ppm, but was more than 21.2 $molm^{-2}yr^{-1}$ at the concentration of 10 ppm of oxygen. The authors suppose that this was caused by hydrogen production in the pits of localized corrosion that occurs in solution with the higher oxygen concentration.
Fujiwara et al. (2001) also observed that for oxygen concentration 100 ppb the production of hydrogen from carbon steels increases with an increase of oxygen concentration. They also suppose as Hara et al. (1992) that this is caused by an increase of the localized corrosion area. But under sufficiently reducing conditions, it has been found that generation of hydrogen tends to increase when the oxygen concentration is lower. It was explained as follows: when a passive film is produced on the surface of carbon steel, the generation of hydrogen extremely decreases to the equivalent corrosion rate of 0.01 $\mu m/y^{-1}$ or less. However, under a very low concentration of oxygen, the passive film cannot be reproduced sufficiently and therefore the

corrosion rate becomes higher. They suppose that air passive film, formed by Fe_2O_3, changes to Fe_3O_4 by the dissolution of Fe_2O_3 as a complex ion $HFeO_2$, which in turn produces Fe_3O_4 by reaction with H^+.

Fujisawa et al. (1997) measured hydrogen production from carbon steel wires in high alkaline non-oxidizing solutions mortar water (pH = 12.6), in aqueous solution saturated with calcium hydroxide (pH = 12.8) and in synthetic bentonite solution (pH = 8) at three temperatures: 15, 30 and 45 ^{o}C. The content of oxygen was below 0.06 mg/l. They observed that hydrogen generation increased with temperature. The hydrogen generation at 15 °C was not detected during a period of 2000 hours, then increased at an almost constant rate with time. At 30 °C hydrogen gas was estimated to be 4 nm/year for 200 hours and then increased to the rate 20 nm/year. The hydrogen production measured at 45 °C was higher at initial period of 1000 hours (corresponding to corrosion rate of 200 nm/yr), but then became lower (not quantified in the paper). They observed a very distinct effect of temperature on hydrogen production. The activation energy of corrosion in alkaline water was about 18 kJ/mol. In alkaline (mortar) water, the corrosion rate decreased with time. In contrast, in synthetic groundwater (pH ~ 8) hydrogen gas was generated at a constant rate (90 nm/year). The difference in behaviour was explained by the fact that in synthetic groundwater, below pH 9.5, no passive film is formed.

Smart et al. (2001) used the similar experimental techniques for measuring of hydrogen production in the artificial KBS TR 36 groundwater water at 30 and 50 ^{o}C as Grauer et al. (1991). He also observed as Grauer et al. (1991) or Simpson and Schenk (Schenk, 1988, Simpson, 1984, Simpson et al., 1985) very high values about 3.3 $mol.m^{-2}.yr^{-1}$ in the beginning of experiments. To investigate the effect of oxide formation on metal surfaces, they artificially covered carbon steel wires with magnetite or carbonate layers. They found that both films were able to reduce the initial burst in the hydrogen production rate that was observed on pickled metal surfaces. The thick magnetite film specimens showed very little corrosion during the first 100 hours. At all times the rates of hydrogen production were below those measured on unfilmed (i.e. pickled) specimens at comparable times. It was found that a more protective layer is formed by magnetite than by iron carbonate.

The addition of 0.1 M $FeSO_4$ in groundwater (Smart et al., 2001) resulted in notably increased long-term hydrogen production rates, compared to KBS TR 36 groundwater. This was explained by the fact that non-protective layer of $FeSO_4$ might be formed on the surface of the carbon steel wires and prevented adherence of protective magnetite layer or alternatively iron sulphate may have caused iron carbonate to precipitate out of the solution, thus leading to a decrease in the pH and formation of a more aggressive environment. Only slight increase of hydrogen production was, however, observed with addition of K_2SO_4. An increase of hydrogen production by addition of $FeSO_4$ could be also explained by reactions of ferrous ions with water leading to hydrogen production. This reaction could also explain a significant decrease of pH observed under an addition of $FeSO_4$ to the groundwater. An increased acidity itself can also lead to increasing corrosion rate and hydrogen production.

The effect of ionic strength and addition of radiolysis products (9 mM NH_3 or 3 mM HNO_3) or of bentonite to groundwater was also investigated in the paper of Smart et al. (2001). It was observed that ionic strength caused a decrease in the hydrogen production during the first 500 hours compared to more dilute solutions, but in the long term (> 1000 hours) the corrosion rate was approximately an order of magnitude greater than in dilute groundwater. A number of explanations of this effect were formulated in the publication of Smart et al. (2001):

- Increased competition between the formation of magnetite and other less protective iron salts, such as $FeCO_3$ or $FeSO_4$

- Increased availability of anions to form more soluble corrosion products, for example $FeCl_2$ instead of $Fe(OH)_2$, and hence reduced ability to form a protective magnetite film
- Incorporation of ions in the magnetite film increasing its conductivity
- Local buffering of pH
- Decrease in the thickness of the protective hard inner magnetite layer due to local buffering of the pH
- Increased conductivity may enable more efficient electron transfer to occur between the carbon steel and the water.

The effect of an addition of NH_3 (9 mM) or HNO_3 (3 mM) was not significant. They also found that the corrosion rate of cast iron compared to carbon steel is lower. The gas generation rate did not increase significantly after removal of the non-adherent corrosion product, suggesting that hard not-removable inner layer provides the majority of the protection.

Smart et al. (2004) measured the rate of generation of hydrogen produced by the anaerobic corrosion of carbon steel wires in contact with bentonite. The results showed that initially (several hours) the anaerobic corrosion rates of carbon steel were higher in bentonite than in an artificial groundwater at a comparable pH (30 μm/year vs 5 μm/year). However, in the long term the anaerobic corrosion rates were similar. They explain it by the incorporation of iron ions in bentonite that cannot be utilized for the formation of protective layers.

2.1.2.2 CORROSION IN PRESENCE OF GEOMATERIALS

Marsh and Taylor (1988) performed laboratory tests of carbon steel corrosion covered with either crushed granite or bentonite paste to depths of 5, 7.5 or 10 cm in synthetic granitic water. Three types of steel were included in the programme: forged steel, cast steel and low carbon forged steel. Average corrosion rates from experiments, which lasted more than 3 years, were in the range 1.7 to 7.7 $\mu m.yr^{-1}$ in contact with bentonite and 19.2 to 26 $\mu m.yr^{-1}$ in presence of granite. The corrosion rate was determined from weight loss measurements. The corrosion rate of the cast steel was 3-4 times less than the forged steel in bentonite, although there was little to distinguish their behaviour in granite. Only general attack occurred in bentonite. Bentonite specimens were covered by an adherent ~ 0.1 mm layer of bentonite + corrosion product which spalled when it dried out. Visually there was a definite colour change in the bentonite approximately 4.5 cm inward, suggesting this marked region became contaminated with corrosion products. Without the presence of oxygen, Marsh and Taylor (1988) strongly suggest that the corrosion rate of carbon steels will be well below 1 $\mu m.yr^{-1}$ (0.2 $mol.m^{-2}.yr^{-1}$) at temperatures below about 50 °C.

Honda et al. (1991) measured the corrosion rate of carbon steel in contact with compacted bentonite. Three specimens with compacted bentonite were placed in a teflon container and filled with water. The bentonite swelled and filled the container. An average corrosion rate was evaluated from the weight loss of specimens. The averaged corrosion rate decreased gradually with increasing test time and was estimated to be in the range 1 to 10 μm/year (0.2 – 2 $molm^{-2}yr^{-1}$) after period 180 days. Corrosion rates in compacted bentonite were approximately one order of magnitude lower than that in bentonite slurry. Corrosion rates in compacted bentonite mixed with synthetic sea-water were about 2 to 4 times higher than that in compacted bentonite mixed with distilled water. Corrosion rates in compacted bentonite mixed with distilled water were independent of the bentonite bulk density in the range of 0.69 -1.32 g/cm^3. On the other hand, corrosion rate in the compacted bentonite mixed with synthetic sea-water

decreased with an increase in bulk density of the bentonite. Authors suppose that corrosion rates of carbon steel in compacted bentonite were controlled by the diffusion of dissolved oxygen in the compacted bentonite. Only magnetite was found in the case of tests with distilled water and siderite was identified on most of the specimens immersed in the compacted bentonite mixed with synthetic sea-water.

Xia et al, (2005) have performed anaerobic corrosion experiments on carbon steel in contact with compacted bentonite Kunigel V1 of different densities of range 0.8 – 1.8 g/cm^3 with samples pre-corroded under aerobic conditions. The corrosion rate observed was about 0.1 μm.y^{-1}. Recently, de Combarieu et al., (2007) have compared the corrosion rate of iron powder under anaerobic condition in the presence or not of clay in solution. The value was about 1.4 μm.y^{-1} with Callovo-Oxfordian argillite contrary to 0.66 μm.y^{-1} without clay. They explained by observation that protective magnetite layer was formed on the surface of iron, while SEM observations showed magnetite formation as isolated crystals in bulk clay.

Kozaki et al. (1994) performed corrosion experiments of an iron foil activated by neutrons. The iron foil was placed between two water saturated bentonite specimens and allowed to corrode at 30 °C for periods of 16 to 63 days. The corrosion rate was determined from measuring of total activity of ^{59}Fe released from the foil. No localized corrosion was observed on the surface of the foil. In all the experiments, the values of the corrosion rates in compacted bentonite were on the order of 1 μm.y^{-1}, and no tendency to decrease in the corrosion rates was observed during the period of 60 days.

Anantamula et al. (1987) measured corrosion rate of carbon steel in the packing mixture of 75 wt% of basalt + 25 wt% of bentonite in water containing only 0.1 mg/l of oxygen at 150 °C. The corrosion rates achieved were in the range 23 – 28 μm.y^{-1} for 1 week experiments and 11 – 14 μm/y^{-1} for 2 week experiments. These values were at least 7 times lower than corrosion rates of the same types of steel in oxic conditions (95-230 μm.y^{-1}).

2.1.3 Conclusions

It follows from this literature review that hydrogen production rate from anaerobic corrosion of iron metals is not a constant value. A very high value about 20 mol.m^{-2}.yr^{-1} can be achieved at the beginning of corrosion until a corrosion layer is formed on the surface of metal. This depends strongly on the conditions of experiments such as: temperature, ionic strength, pH of water, or concentration of oxygen in groundwater. In particular, corrosion rate has been shown to increase with the presence of bentonite, though no clear explanation is given so far. It follows from this literature review that after some time corrosion rate will decrease to lower values, certainly below 5 μm/yr corresponding to hydrogen production rate lower than 1 mol.m^{-2}.yr^{-1}. Some of the experimental results, even suggest that corrosion rate in steady state in anaerobic conditions could be well below 1 or even 0.1 μm.y^{-1}/yr (0.02 – 0,2 mol.m^{-2}.yr^{-1}). The experiments reviewed, however, have not been carried out in strictly defined conditions concerning the content of oxygen in water. The results can be doubted therefore from the point that corrosion layers formed on the surface of metal could be more protective than the corrosion layers formed in a repository conditions due to higher content of oxygen in groundwater.

2.2 IRRADIATION

Within geological disposal facilities, iron or carbon steel components (radioactive waste containers, liners...) will be exposed simultaneously to water and radiation as their

environment (host-rock, bentonite...) resaturates. Corrosion processes and water decomposition under radiation will generate gases, mainly hydrogen. Actually, radiolysis of water will occur and produce both radicals and molecular products which could influence corrosion processes. The understanding of the global system behaviour is a prerequisite to assess the gas production rate, which is one of the input data for modelling hydrogen transport in a repository.

This chapter is devoted to the state of the art regarding the production/consumption of gas by corrosion under irradiation. However, there are very few published papers directly related to this issue and the papers which deal with connected topics are often not easily valuable with this perspective. Thus, the following focuses first on works addressing radiolysis of solutions and then corrosion under irradiation.

It is worth mentioning that the irradiation conditions expected in a deep underground repository are strongly dependent on the waste types and on the facility design.

2.2.1 Radiolysis of solutions

2.2.1.1 Pure water radiolysis

When exposed to radiation (α, β, γ, recoil nuclei), water molecules are exited and ionized, and pure water can degrade as follows:

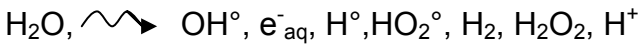

Where species noted ° are radicals and e^-_{aq} corresponds to a solvated electron.

Nota: O_2 is not a primary radiolysis product; it is formed by recombination between hydrogen peroxide and OH°.

The yield of production for each of these species (primary products of radiolysis) depends on the nature of the radiation (Pastina et al., 1999; Wasselin-Trupin, 2000) (Table 3). Actually, under continuous radiation conditions, the concentrations of these radiolysis products depend on LET values. The Linear Energy Transfer (LET), corresponding to the loss of energy by unit length in the medium, depends on the type and energy of the ionizing particles. The LET of high energy photons (such as gamma rays) is 0.2 keV/µm, while for alpha particle the LET can reach 200 keV/µm (Pastina et al., 1999). For high LET values, radicals yields are low and molecular species yields are high (Allen, 1961), while for low LET, radicals are preferentially formed.

Radiation	G(-H2O)	G(e-)	G(OH°)	G(H°)	G(H2)	G(H2O2)	G(H2O)
Gamma rays	1.08	2.63	2.72	0.55	0.45	0.68	0.008
Alpha rays	3.9	0.33	0.3	0.1	1.8	1.67	0.13

Table 3: Yields (number of molecules produced or consumed per 100 eV of adsorbed energy) of primary species (Pastina, 1997)

The primary products undergo reactions (Ershov et al., 2008) with each other resulting in steady-state concentrations of both radicals and molecular species depending on dose rate,

temperature and solution composition. When irradiated with low LET, such as X-rays or gamma rays, pure degassed water gives almost no products (because of radical recombination's, the amount of these products remains at a very low steady state concentration). For high LET such as alpha rays, pure water decomposition occurs with the formation of hydrogen and hydrogen peroxide. When water contains oxygen, decomposition occurs whatever the LET value. If hydrogen is added to aerated water, the water decomposition is suppressed. This behaviour is linked to the series of reactions involved in the chain reaction proposed by Allen (Allen, 1961) which can be summarized as:

$OH° + H_2 \rightarrow H° + H_2O$

$H° + H_2O_2 \rightarrow OH° + H_2O$

$H_2 + H_2O_2 \rightarrow 2\ H_2O$

2.2.1.2 INFLUENCE OF EXPERIMENTAL CONDITIONS

The steady state concentration of a radiolysis product will depend on its radiolysis production rate (constant at a constant dose rate) and on decomposition rates which are very sensitive to aqueous environment characteristics such as pH, temperature and chemical additives (Buxton et al., 1988). Once generated, the primary products undergo further chemical reactions with each other, with water molecules and with other chemical species present in solution (such as pH- or redox-controlling agents). Therefore, the solution chemistry would change with time. The presence of dissolved species or a change in chemical environment affects the concentration of H_2O_2 and H_2 mainly through interactions with radicals e^-_{aq} and OH° (Ross et al., 1979, Lapuerta et al., 2007).

2.2.1.2.1 Dose rate

In the beginning of the exposure, the amount of radicals increases with radiation dose rate. But, because of the differences in kinetics of recombination reactions (Ross et al., 1994), a high dose rate induces an increase of molecular products concentration, a decrease of radicals amounts and finally should conduct to a marked water decomposition. Joseph et al. (2008) have shown that for a given pH the steady-state concentrations have a square root dependence on dose rate.

2.2.1.2.2 Temperature

The diffusion in solution of primary radiolysis products is enhanced by temperature. Therefore, for high temperature, radicals diffuse in solution and the occurring of recombination reactions decrease. Consequently, the amount of radicals is globally higher for high temperature (Elliot, 1994

2.2.1.2.3 Solution composition

If water contains few ppm of dissolved oxygen, the reducing species e^-_{aq}, H°, are rapidly converted to O_2^- and $HO_2°$ respectively. In the case of oxygenated water, the concentrations of H_2 and H° are decreased, Allen's chain is disrupted and water decomposition occurs with production of O_2, H_2 and H_2O_2. At pH 6, for a dose rate of 25Gy/s (gamma rays), the steady-state concentration of H_2 and H_2O_2 in aerated solutions reached respectively 2.6 10^{-5}mol/l and 9 10^{-5}mol/l, while it remains below the detection limit (3 10^{-6} mol/l) in deaerated solutions

(Joseph et al., 2008). The presence of dissolved O_2 while radiation fields endures, will lead to a significant increase in the production of radiolytic oxidant.

The steady-state concentrations of deaerated water decomposition products are nearly independent of pH in the range 5-8. However raising pH above 10 significantly increases steady-state concentrations in H_2O_2 and H_2 (at the expenses of OH° and e^-_{aq} concentrations) as well as the time to reach steady-state. H_2O_2 and H_2 concentrations were below detection limit at pH 6 and 8.5; while at pH 10.6 [H_2O_2] was found to be $\sim 3\times10^{-5}$ mol dm^{-3} and [H_2] $\sim 2\times10^{-4}$ mol dm^{-3} after a 5 h irradiation (2.5Gy/s). At pH>10, the production of oxygen becomes significant but at a finite rate (Joseph et al., 2008; Yakabuskie et al., 2010).

When carbonate is present, as in bentonite porewater (Appendix 1), OH° will be quantitatively converted into CO_3^-°, this being also a strong oxidant (E_0 (NHE) = 1.9V and 1.59V respectively) (Nielsen et al., 2008). Fattahi et al (1992) have reported an increase (factor 2) of hydrogen peroxide production for clay solution compared to pure water.

2.2.2 Radiolysis modelling

Different softwares are available for numerical simulations of solutions radiolysis. Facsimile (Chance et al., 1977), Maksima-Chemist (Carver et al., 1979) and Chemsimul (Rasmussen et al., 1984) are the most used. The models are underlain by a set of chemical reactions taking place in pure water and aqueous solutions between the different species produced by irradiation, together with their kinetics constants and the radiation chemical yields of radiolysis products.

Kinetics constants are gathered in different data bases (Ross et al., 1994; Elliot et al., 2009).

An example of radiolysis modelling with Chemsimul software, using the RATES data base (Ross et al., 1994) completed by data from Buxton et al. (1988) and Ershov et al. (2008) - see Appendix 2 for an example of input data - is presented on figures 3 and 4. In pure deaerated water, the production of hydrogen increases with the dose rate and the duration of radiation (total dose). In presence of carbonate, hydrogen production increases (Fig. 4).

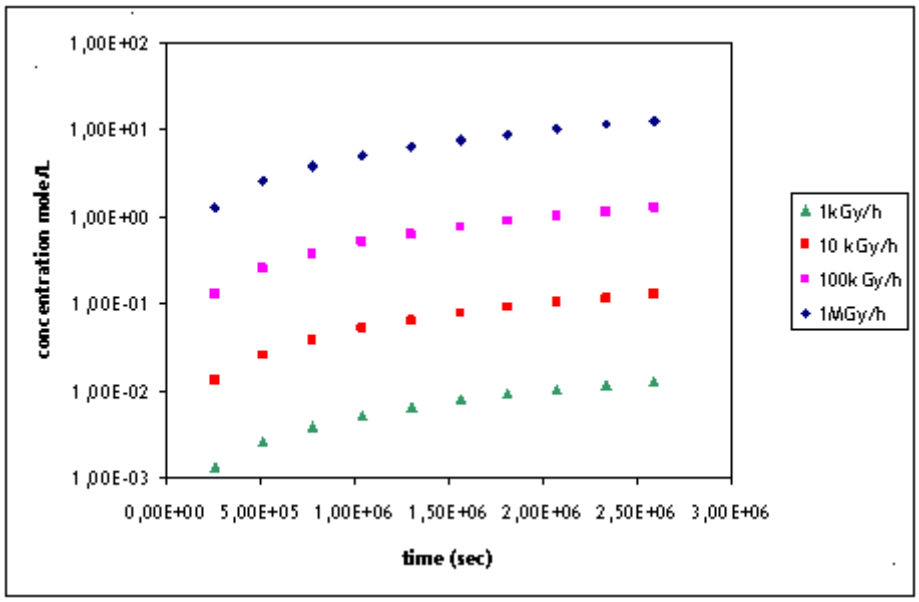

Figure 3: Hydrogen production by irradiated water as a function of dose rate

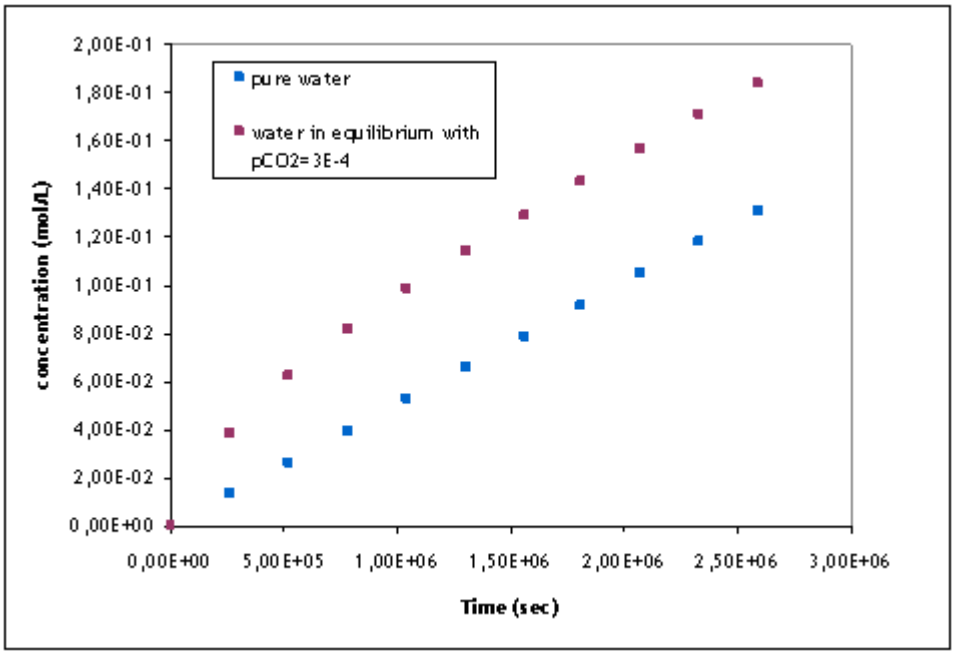

Figure 4: Influence of carbonate on hydrogen production – dose rate = 10kGy/h

2.2.3 Influence of radiation on corrosion

Water radiolysis produces both oxidizing (OH°, H_2O_2) and reducing (H_2, e^-_{aq}) species and can dominate redox conditions and strongly influence the corrosion kinetics of materials in contact with water (Joseph et al., 2008). For a reactive material such as carbon steel, the redox conditions are established by the interactions between radiolysis products, steel surface and the corrosion products produced by the corrosion processes (Joseph et al., 2008).

Consumption of a radiolysis product, for example H_2O_2 during corrosion, can influence the concentrations of other radiolysis species by disturbing the steady-state balance between them. Corrosion also produces soluble iron species (Fe II and Fe III) which can react with water

radiolysis products and interfere with the steady-state balance between radiolytic species and modify the composition of the corrosion surface.

An attempt to represent this synergistic circuit is shown in Fig. 5.

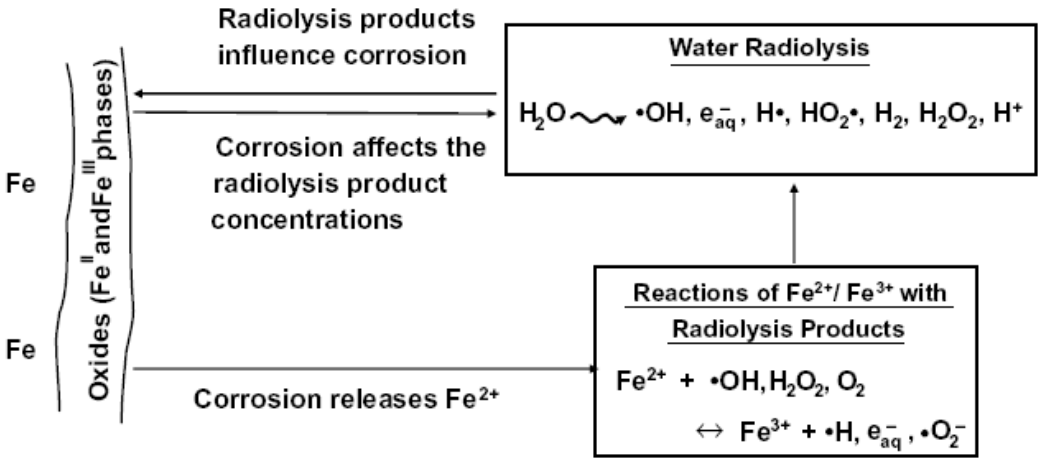

Figure 5: An example of reactions occurring at the interface of carbon steel solution under irradiation (from Zhang et al., 2007).

Literature reports some studies on the corrosion processes in primary coolant water of nuclear power plants (Daub et al., 2008; Pastina et al., 1999). To limit the corrosion processes in primary coolant water in nuclear reactors, an excess of molecular hydrogen is introduced in this water. Molecular hydrogen will prevent the accumulation of oxidants products such as oxygen and hydrogen peroxide, which are responsible for the corrosion of the primary system (Pastina et al., 1999). The molecular hydrogen participates to a chain reaction which recombines H°, OH° and H_2O_2 back to water (Allen chain). Therefore, oxidant species content decreases and the corrosion is reduced.

Several authors have put in evidence enhanced corrosion of different materials as ceramics, zircaloy and other metals under charged particle radiations (Burns et al., 1983; Ishigure et al., 1980; Lapuerta et al., 2005; Lillard et al., 2000).

The influence of ionizing radiation on corrosion of metals has been studied only to a limited extent, and mechanisms by which radiations affect corrosion kinetics have not been established (Daub et al., 2009). The observed effects of ionizing radiation on the corrosion of metals are sometimes conflicting and many key questions remain open.

2.2.3.1 Influence of dose rate

Fujita et al. (Fujita et al., 2000; Fujita et al., 2001) have observed a corrosion rate in pure deaerated water under a dose rate of 0.55kGy/h for 300, 600 and 900h six times larger as that under a non-irradiated condition. An experimental study (Marsh et al. 1988) on the corrosion of carbon steel in presence and absence of radiation (dose rate up to 10^3 Gy/h) has been conducted in synthetic granitic waters (pH = 9.4). Without irradiation, the rate of general corrosion was less than 0.1 µm/y. In the same environment, with a maximum gamma dose rate of 10^3 Gy/h, the general corrosion rate was fairly constant at 3 µm/y at least up to 5236 h (duration of the experiment). As on unirradiated samples, no localized corrosion was observed.

Smart et al. (2008) have also found that radiation (11 Gy/h, 300 Gy/h) enhanced the corrosion rates of carbon steel wires in contact with 2 synthetic groundwaters (equilibrated with granite and with bentonite, anaerobic conditions). The corrosion rate value estimated on the basis of hydrogen release is closed to values obtained by Marsh et al. (1988) (3 µm/y compared to less than 0.1µm/y without radiation). No localised attack was observed.

2.2.3.2 INFLUENCE OF SOLUTION COMPOSITION

Lapuerta et al. (2005) have observed that under irradiation, corrosion of iron in pure water is enhanced when oxygen is dissolved in solution (corrosion is twice more significant in aerated medium than in deaerated one). Marsh et al (1988) have compared steel corrosion in synthetic seawater under and without irradiation. Unirradiated experiments have been conducted for periods up to 5000 h; the general corrosion rate obtained settled at 6 µm/y and no localized attack is developed. The irradiated tests, conducted for periods up to 400 days, showed appreciable acceleration in the rate of corrosion with the weight loss measurements indicating corrosion rates exceeding 100 µm/y in some tests at the highest dose rate (1.5 10^3 Gy/h). Visual inspection showed that much of the corrosion at all three dose rates (3, 35 and 1.5 10^3 Gy/h) had occurred as patches of attack on the edges of the specimens, which suggests that it may be associated with some metallurgical inhomogeneity in the steel. In some cases these areas had penetrated up to 0.5 mm and the variability in the number and size of these local sites accounts for the large scatter in the weight loss data.

At last, Smart et al. (2008) reported a more pronounced enhancement of the corrosion rate under radiation for “granitic water“than for bentonite water. A 30 fold increase was observed in granitic water while for bentonite water (higher ionic strength, higher initial pH value), the radiation-induced enhancement was 10-20 times. Nevertheless, the authors observed that hydrogen generation rate decrease over time.

Daub et al. (2009) have shown that the corrosion observed for a pH = 10.6 under gamma-irradiation at room temperature, could be reproduced well by exposing the steel to hydrogen peroxide solutions. These authors observed that the addition of H_2O_2 in multiple steps (progressive addition), matches the change in corrosion potential under irradiation. In the conditions of the experiment, Daub et al. (2009) concludes that H_2O_2 is the key radiolysis product. But, Lapuerta et al. (2007), who have conducted protons irradiation experiments have shown that radicals produced by water radiolysis participate to the corrosion processes, together with hydrogen peroxide.

In many cases, the main corrosion product of carbon steel in contact with water is magnetite, Fe_3O_4, but there was some evidence of higher oxidation state oxyhydroxides (Fe_2O_3, FeOOH) under high dose rate (Daub et al. 2009; Xu et al., 2008). Smart et al. (2008) mentioned that the corrosion product formed under high dose rate (300Gy/h) has a different colour to the specimen obtained at 0 and 11Gy/h. Fujita et al. (2000) have observed through X-Ray Diffraction analysis a preferential dissolution of a specific (110) plane, which potentially triggers an occurrence of the pitting corrosion and an incipient crack.

2.2.3.3 CORROSION IN ATMOSPHERIC CONDITIONS

Lapuerta et al. (2005; 2007; 2006) have studied corrosion of iron under proton radiation in atmospheric conditions for different humidity contents. Without radiation, the corrosion kinetics is maximum for a relative humidity of 80-90%, while under radiation, the maximum of corrosion is observed for a humidity of 45%. For higher humidity content, the corrosion rate decreases. Lapuerta et al. (2007) conclude that radiation influences corrosion only when water (vapour) and oxygen are simultaneously present.

2.2.4 Conclusions

Studies devoted to corrosion under radiation tend to indicate that the corrosion of carbon steel is enhanced under irradiation. But uncertainties still remain about the processes as well as the factor of enhancement, which may range between about 1 and 30. For example, no unanimity was obtained regarding the state of the surface of carbon steel corroded under irradiation: is it generalized or localized corrosion? Authors have observed the formation at the interface steel/solution of magnetite together with oxy-hydroxides. It would worth examining the influence of this last oxide (structure, composition) on the corrosion rate. Besides, no specific data were reported on the redox potential evolution during experiments. At last, the behaviour of hydrogen (production/consumption) as well as the influence of dissolved species (carbonate, chloride…) on this behaviour and on corrosion under radiation has not been addressed. More generally, there is a need for a better understanding of corrosion and hydrogen production/consumption processes under radiation, so as to improve the assessment of intensity and duration of radiation effects.

3 Experimental program

3.1 NRI EXPERIMENTS

3.1.1 Equipment for measuring of hydrogen evolution from Carbon steel in anaerobic box

Equipment for measuring hydrogen evolution from carbon steel in anaerobic box has been based on equipment used before in NF-PRO project for measuring corrosion rate of carbon steel. This equipment is described elsewhere (Vokál et al., 2007). In this project the equipment was significantly modified to carry out the experiments in our anaerobic box. For most of experiments a cell shown on Fig. 6 was used. The 10 samples of dimension 7 x 7 cm (surface 99.76 cm2) with hole samples were separated by Teflon distance inserts (5 mm). Steel plates were immersed in approximately 2 l of synthetic bentonite water solution.

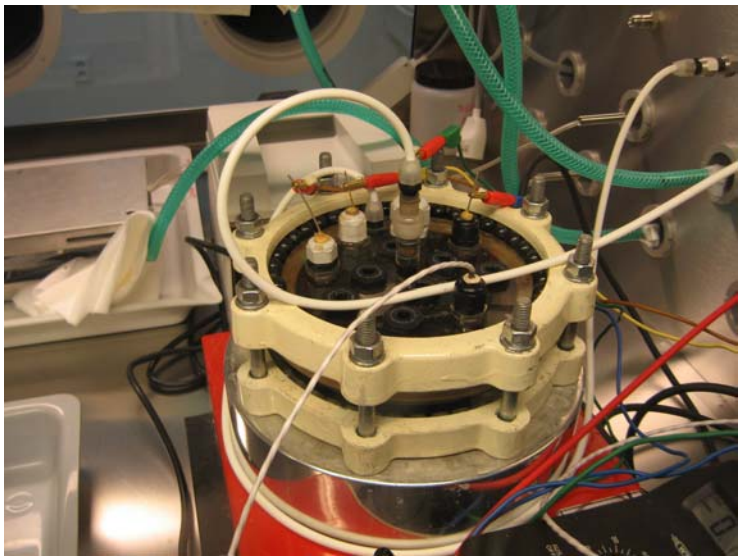

Figure 6: Equipment for measuring hydrogen evolution in anaerobic box

The composition of synthetic bentonite pore water corresponded to the composition of sodium bentonite Volclay KWK 20-80 of a density of 1600 kg.m-3 (Table 4). It was prepared according to the recipe prepared on the basis of the calculations carried out in the NF-PRO project (Vokál et al., 2007).

Table 4: Composition of bentonite synthetic water

Table 1			
ρ_B [kg.m^{-3}]	1300	1600	1900
log(P_{CO2}) [bar]	-3,42	-3,47	-3,65
pH	8	8	8
I [mol.l^{-1}]	0,26	0,29	0,33
c(Na) [mol.l^{-1}]	1,83.10^{-1}	2,07.10^{-1}	2,54.10^{-1}
c(K) [mol.l^{-1}]	2,7.10^{-3}	3,1.10^{-3}	3,7.10^{-3}
c(Mg) [mol.l^{-1}]	1,0.10^{-2}	1,2.10^{-2}	1,5.10^{-2}
c(Ca) [mol.l^{-1}]	9,2.10^{-3}	9,8.10^{-3}	1,2.10^{-2}
c(Sr) [mol.l^{-1}]	8,1.10^{-5}	8,6.10^{-5}	1,1.10^{-4}
c(Cl) [mol.l^{-1}]	1,81.10^{-2}	6,18.10^{-2}	1,7.10^{-1}
c(SO_4) [mol.l^{-1}]	1,02.10^{-1}	9,5.10^{-2}	7,1.10^{-2}
c($C_{anor.}$) [mol.l^{-1}]	8,9.10^{-4}	8.10^{-4}	5,5.10^{-4}
c(F) [mol.l^{-1}]	2,2.10^{-4}	2,2.10^{-4}	1,9.10^{-4}
c(Si) [mol.l^{-1}]	1,8.10^{-4}	1,8.10^{-4}	1,8.10^{-4}

Composition of carbon steel of Czech standard ČSN 11321 is given in Table 5.

Table 5: Composition of carbon steel

Element	C	P	Mn	S
%	0.1	0.035	0.45	0.035

The content of oxygen in the anaerobic box was lower than 0.1 ppm. Pt, Au and silver chloride reference electrodes were used for Eh measurements. A reference electrode had to be prepared by coating Ag wire with silver chloride, because commercial reference electrodes could not be used due to the significant changes of electrolytes inside the electrodes. The experiments were carried at various temperatures in the range 40 – 70 °C and controlled by a TDC 2 Temperature Controller with a Watlow series 988 PID control unit. The experiments lasted 30 days. During the experiments hydrogen evolution rate, temperature, pH and Eh were measured.

3.1.2 Equipment for Measuring of hydrogen migration through compacted bentonite with and without backpressure

Devices for measuring hydrogen migration through compacted bentonite are shown in Fig. 7 and 8. In the first device, change of volume caused by hydrogen evolution was measured using

a LVTD Displacement Transducer and in the second one, by displacement of piston of Digital Compression Testing Machine, which held a constant backpressure.

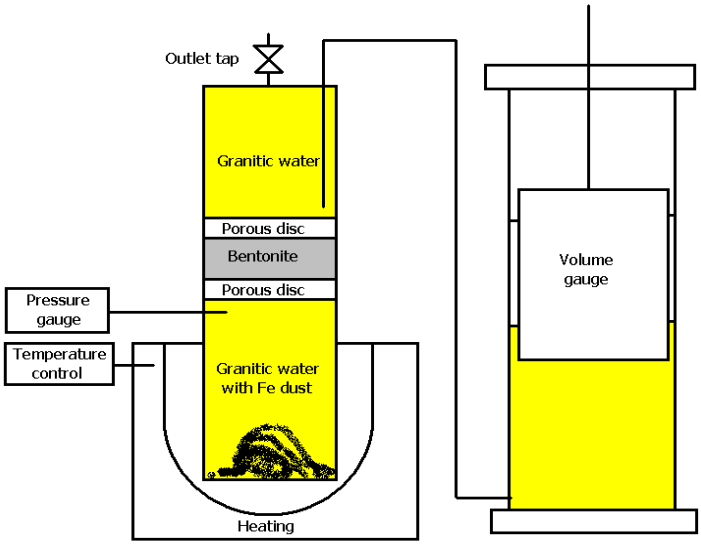

Figure 7: Scheme of device for measuring hydrogen migration without backpressure

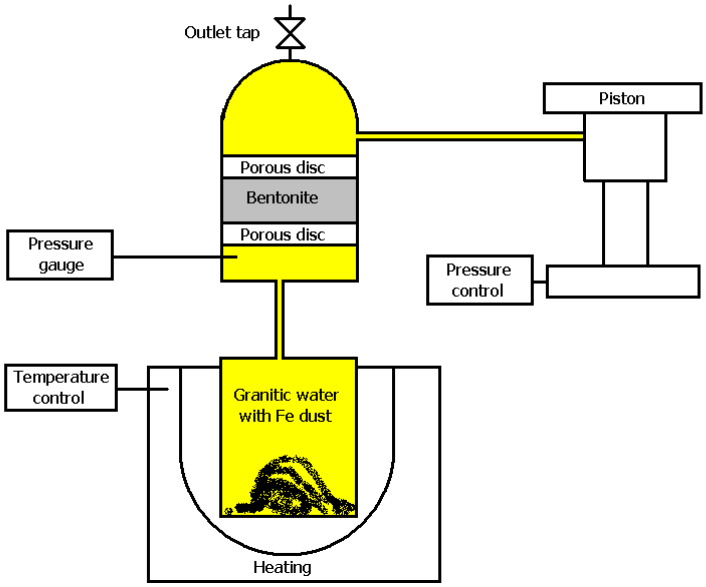

Figure 8: Scheme of device for measuring hydrogen migration with backpressure from compression machine

Bentonite samples made of Wyoming type bentonite (Volclay KWK-20-80 or Voltex) or Czech bentonite from deposit Rokle, were prepared using a Compression Testing Machine at pressure 15 MPa until outflow of water from the sample. This way to get saturation enabled also to measure permeability of bentonite samples. The diameter of samples were 30 mm and thickness 15 mm. The density ranged from 1200 to 1750 kg m^{-3}. Picture of a sample of bentonite from Rokle deposit is shown in Fig. 9.

Figure 9: Sample of saturated bentonite Rokle for measuring hydrogen migration

The experiments were carried out at various temperatures controlled by OMRON E5CN temperature controller. All parameters were monitored using Data logger PUI 03 – 54 from DataCon MSI. Various iron powder samples were used for experiments. But only iron of very high purity (>99.5 %) and high surface (0.2 m^2/g) provided hydrogen evolution rate suitable for performance of hydrogen migration experiments (Riede-daHaen, Cat. 12311 or 000170 Alfa Aesar). 5 – 30 g of iron powder was used in experiments.

A large number of experiments failed due to a multitude of reasons, mostly due to the leakage of hydrogen, use of unsuitable iron powder, consumption of total amount of water in reactor for hydrogen evolution, etc. Some of experiments with iron powder were also carried without bentonite to find corrosion rate without the bentonite, but these experiments failed because iron was embodied by hydrogen and the hydrogen evolution rate was significantly slowed down.

The experiments that have been carried out successfully and the results obtained will be presented and discussed in FORGE WP2 Deliverable 2.2.

3.1.3 Equipment for measuring hydrogen evolution rate in contact of carbon steel with bentonite

A special corrosion chamber has been developed and manufactured for measuring hydrogen evolution rate under contact with compacted bentonite. The corrosion chamber is shown in Fig. 10. A detailed technical description of the corrosion chamber will be described later in the final report. The chamber enables in addition to measuring change of volume using LVTD Displacement Transducer Sensor to measure swelling pressure and pressure induced by hydrogen evolution. The samples of compacted bentonite, prepared using compression testing machine, were saturated under high pressure using Haskel Pump, Model MS-21. This enables also to carry out experiments under increased backpressure.

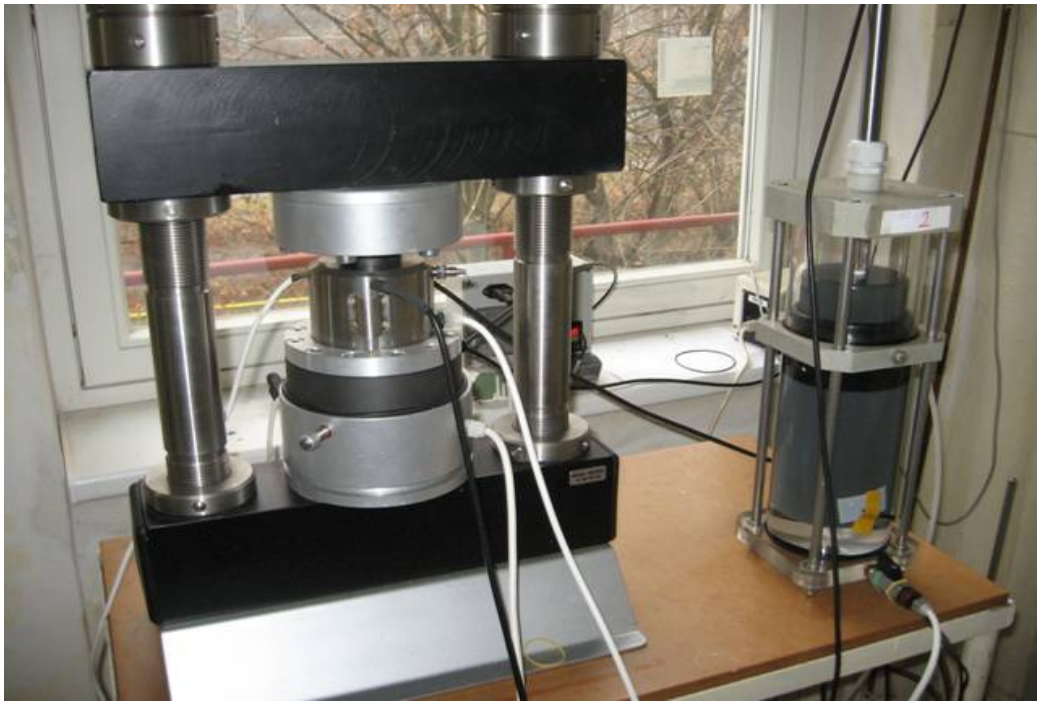

Figure 10: Corrosion chamber for measuring hydrogen evolution from carbon steel in contact with compacted bentonite.

3.1.4 Equipment for measuring hydrogen evolution under irradiation (cooperation with IRSN)

The corrosion cell for measuring hydrogen evolution under radiation or under other remoted sites (e.g. anaerobic box) or in situ experiments was developed and manufactured. The scheme of the corrosion cell is given in Fig. 11. It uses the same principle of measuring volume change with LVDT Displacement Tranducer as above described devices. The experiments without radiation and preliminary experiments under Co(60) were carried out also in NRI. The cell was provided to IRSN for further experiments under radiation. Due to problems with leakage of hydrogen, it was necessary several times to modify sealing system of the corrosion cell against hydrogen leaking.

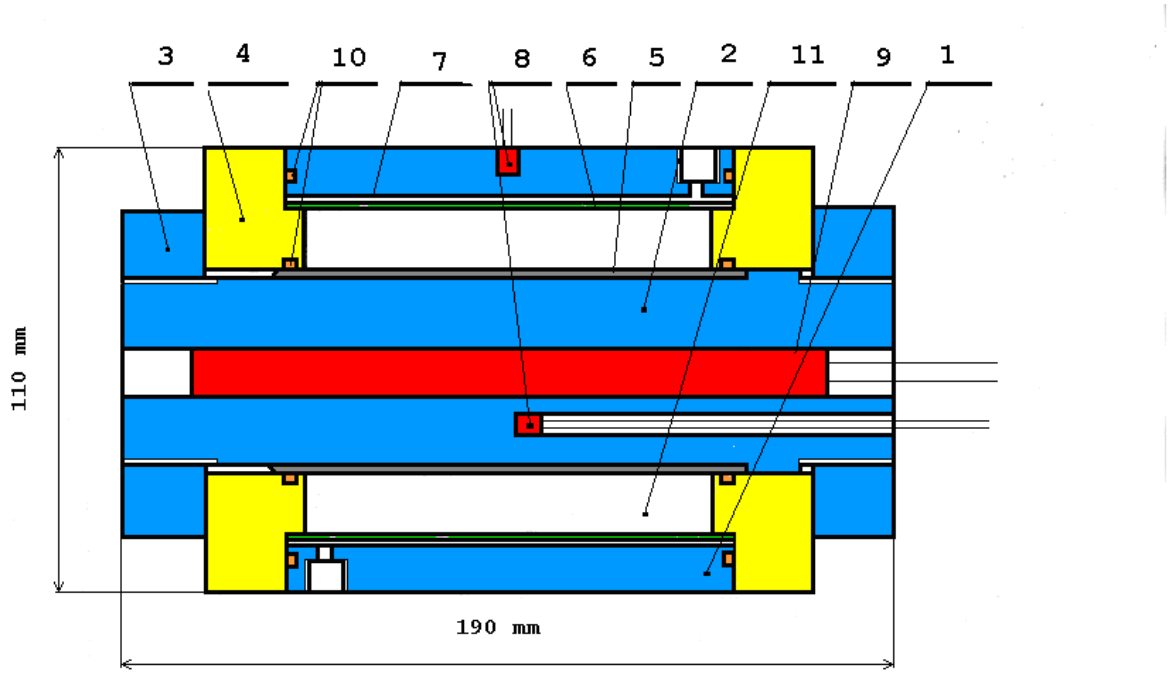

Figure 11: The corrosion chamber for measuring hydrogen evolution under radiation before modification.

1. **Chamber case**
2. **Chamber body**
3. **Nuts**
4. **Cover**
5. **Sample in the form of a tube**
6. **Filtration textile**
7. **Watering tube**
8. **Temperature sensor**
9. **Heater**
10. **Sealing O circles**
11. **Solution, bentonite or other material**

Picture of the cell after irradiation is shown in Fig. 12.

Figure 12: Picture of corrosion cell after irradiation by Co-60

3.2 IRSN EXPERIMENTS

IRSN experimental program defined in the FORGE project WP2 aims at quantifying the gas production by aqueous carbon steel corrosion under irradiation. A comparison with hydrogen released by corrosion without radiolysis will help assessing the effect of radiation on corrosion processes.

The above literature review has shown that according to the composition of the solution, gas releases and steel corrosion may vary. Particularly, carbonate ions can play an important role in corrosion processes through the formation of carbonate radical, which is strongly oxidant. In order to be in conditions representative of a high level waste disposal in clayey geological formation, the solution used for our experiments will be characteristic of clay porewater; bentonite porewater (appendix 1) would help for comparison purposes with NRI results

This study will be conducted with the device developed by NRI (see chapter 3.1 related to NRI experiments). The whole cell (containing both steel and solution) will be irradiated. The gas produced by corrosion (H2) and solution radiolysis (H_2, O_2) will be analyzed continuously. At the end of the experiment, the device will be dismantled and the solution analyzed (H_2O_2, Fe, pH…). If possible, carbon steel will be analyzed, in order to determine the weight variations and observed (Scanning Electronic Microscopy) in order to determine the nature of the corrosion layer.

These experiments required numerous tests for the validation of the experimental set up with the strong constraints of i) online gas measurement by gas chromatography and ii) irradiation conditions. Various difficulties have occurred (gas and liquid leakages, uneasy dismantling leading to bias…) so that, a part from the definition by calculation of the irradiation conditions, this report mainly describes the outlines of IRSN objectives in terms of plan of experimental works.

3.2.1 Definition of the irradiation conditions

Irradiation experiments will be performed in IRMA (IRradiation MAtériaux) facility (Fig. 13). This facility is devoted to the study of the radiation-matter interactions and more specifically to the behavior of materials and devices under γ radiation. Because of its large volume ($24m^3$), this facility allows a wide range of measures considering different geometries.

Four cylindrical sealed sources (^{60}Co) with different activities are available for irradiation (see values in table 6). Their diameters are 10 mm and their lengths vary between 229 and 452 mm. The dose rate available is comprised between 5 µGy/h and 15 kGy/h.

Figure 13: IRMA facility

Table 6: Characteristics of ^{60}Co sources

Source Reference	1	2	3	4
Activity (TBq)[1]	89.57	86.51	161.97	163.80

The conditions of irradiation (number and position of the sources versus cell, duration of irradiation…) were chosen in order to have the maximum of energy deposited in the solution and to have a homogeneous distribution of energy in solution.

Two softwares (Mercurad, MNHX) were used to determine the amount of energy deposited in a sample as a function of the energy of the incident particles, the number and position of ^{60}Co sources. The thickness of the different components used (stainless steel, carbon steel) was fixed and the volume of solution introduced in the cell was 310.896 cm^3 (Fig. 14).

[1] Values calculated at the date of April 21st , 2010, ^{60}Co period = 5,2714 years

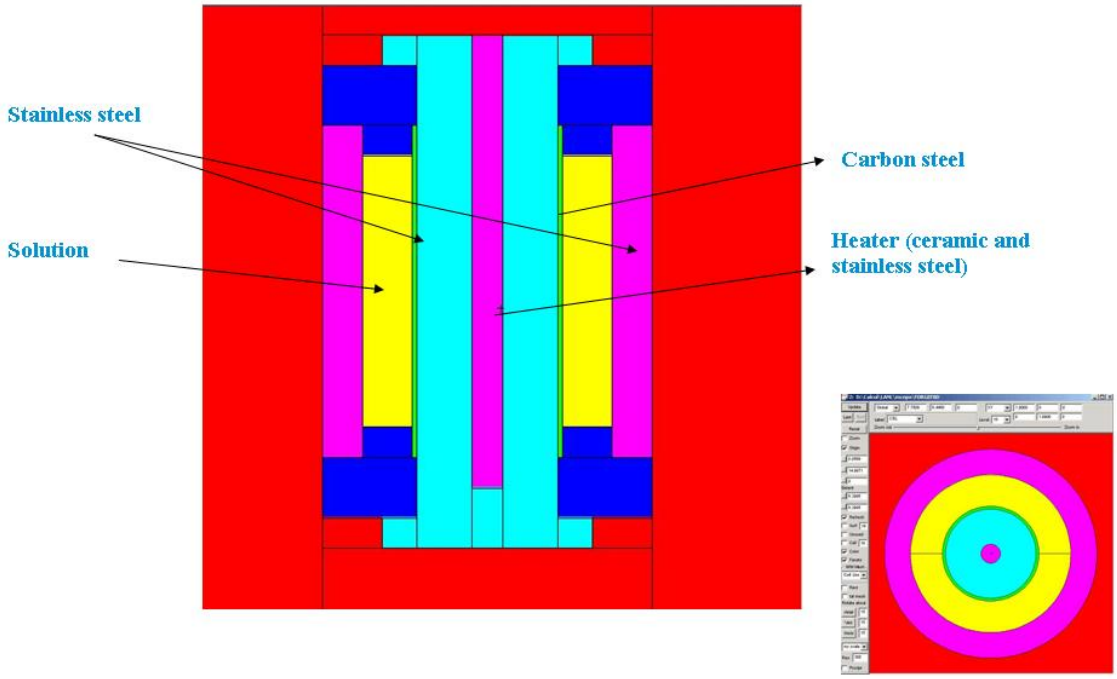

Figure 14: Representation of the structure of the cell

The irradiation conditions allowing the higher gas production rates and a uniform deposit of energy in solution were obtained with two sources disposed at a distance of 150 mm from the cell. In these conditions, the total energy deposited 8.94 10^{11}MeV/s corresponds to a total absorbed dose of 1.66 10^{3} Gy/h. These conditions were chosen for the first experiments to facilitate the measurements by the production of significant amounts of hydrogen easily measured and to elucidate the influence of solution characteristics on the gases production. More realistic conditions close to those predicted in a radioactive waste disposal will be used for the following experiments.

3.2.2 Analyses

On-line measurements of hydrogen and oxygen released will be made by gas chromatography (Varian GC 450, equipped with a pulsed discharge helium ionization detector). The cell is placed inside IRMA facility for irradiation, while the analysis equipments are outside of the irradiation zone and connected to the cell by a stainless steel tube of 10 m long.

Hydrogen peroxide will be measured after the dismantling of the cell by spectrophotometry according to Ghormley method.

At the end of the experiment, the solution composition will be determined and compared to the initial one (pH, cations and anions, iron species). The carbon steel will also be observed and characterized.

3.2.3 Implementation of input files in Chemsimul for radiolysis simulations

The experimental data (H_2, O_2 and H_2O_2) will be compared to modelling data obtained with the Chemsimul software. If a good agreement is obtained between both experimental and

modelling results, it will be possible to examine through simulations the influence of different parameters such as pH, presence of oxygen, solution composition (carbonate, bicarbonate, chloride, sulphate…) and to identify the key parameters governing the corrosion under radiation and thus the gas release.

3.2.4 Experimental plan

3.2.4.1 DEFINITION AND TESTS OF THE EXPERIMENT

The feasibility of such online measurements by gas chromatography will be tested on the basis of corrosion experiments without irradiation. In particular, it is necessary to test the capacity of the gas chromatography device to detect and quantify the gas release.

The conditions of measurements will be defined and the sensibility of GC determined. On a same way the sensibility of the method used for H_2O_2 detection will be tested in the conditions of our experiments (saline solutions, presence of iron species).

3.2.4.2 TIME LIMITED IRRADIATIONS (<2 MONTHS)

These experiments will allow quantifying hydrogen production when corrosion and radiolysis occurs simultaneously. A first test will be carried out with pure water in contact with carbon steel.

In a second experiment, the influence of solution composition on this production rate will be studied in order to assess the possible specific roles of some species (carbonates, iron corrosion products, organic components...).

In both cases, both solids and solutions will be analysed.

3.2.4.3 LONG TIME IRRADIATION (> 1 YEAR)

This experiment will allow examining the evolution of gas production with time, the influence of lower dose rates, and to verify if a steady-state is obtained for gas amounts.

4 References

Allen, A.O., 1961, The radiation chemistry of water and aqueous solutions, *in* Nostrand, V., ed.: New York.

Anantamula R.P., Delegard C.H., Fish R.L., 1984, Corrosion behaviour of low-carbon steels in Grande Ronde Basalt groundwater in the presence of basalt-bentonite packing, *Scientific Basis for Nuclear Waste Management VII, Mat. Res. Soc. Sym Proc.* Vol. 26, p.113

Burns, W.G.M., W. R.;Walters, W. S., 1983, The [lambda] irradiation-enhanced corrosion of stainless and mild steels by water in the presence of air, argon and hydrogen: Radiation Physics and Chemistry (1977), v. 21, p. 259-279.

Buxton, G.V., Greenstock, C. L.,Helman, W. P., Ross, A. B., 1988, Critical Review of rate constants for reactions of hydrated electrons, hydrogen atoms and hydroxyl radicals OH°/O˙ in Aqueous Solution: *Journal of Physical and Chemical Reference Data*, v. 17, p. 513-886.

Carver, M. B., Henley, D.V. Chaplin, K.R., 1979, Maksima-Chemist a program for mass action kinetics simulation by automatic chemical equation manipulation and integration usiong stiff techniques, AECL-6413, Chalk River Nuclear Laboratories

Chance ,E.M., Curtis, A.R., Jones,I.P., Kirby, C.R., 1977, Facsimile: a computer program for flow and chemistry simulation, and general initial value problems, AERE-R 8775 Report, AERE, Harwell.

de Combarieu G., Barboux P., Minet Y., 2007, Iron corrosion in Callovo-Oxfordian argillite: Form experiments to thermodynamic/kinetic modelling, *Physics and Chemistry of the Earth* 32, 346-358

Daub, K.Z., X.; Noël, J. J.;Shoesmith D.;Wren, J. C., 2008, Effect of gamma radiation on steel corrosion, *in* Curran Associates, I., ed*., 9th Annual Conference of the canadian Nuclear Societey and 32nd CNS/CNA Student Conference*: Toronto -Ontario, CANADA.

Daub, K.Z., X.; Noël, J. J.;Wren, J. C., 2010, Effects of [gamma]-radiation versus H2O2 on carbon steel corrosion*: Electrochimica Acta,* vol55,8,2767-2776

Dunn D.S., Cragnolino G.A., Sridhar N., 2000, An Electrochemical Approach to Predicting Long-Term Localized Corrosion of Corrosion-Resistant High-Level Waste Container Materials, *Corrosion-January*, Vol. 56, No.1, 90-104

Druyts F., Kursten B., Van Iseghem P., 2001, Corrosion Evaluation of Metallic Materials for Long-Lived HLW/Spent Fuel Disposal Containers, *Final report to EDF for the period 1996-1998*, SCK.CEN, R-3533, May

Elliot, A.J., 1994, rate constants and G-values for the simulation of the radiolysis of light water over the range 0-300°C, *in* 11073, A.-. ed.

Ershov, B.,G.,Gordeev, A.V., 2008, A model for radiolysis of water and aqueous solutions of H_2, H_2O_2 and O_2: *Radiation Physics and Chemistry*, v. 77, p. 928-935.

Fattahi, M., Houée-Levin, C., Ferradini, C., and Jacquier, P., 1992, Hydrogen peroxide formation and decay in [gamma]-irradiated clay water: International Journal of Radiation Applications and Instrumentation. Part C. Radiation Physics and Chemistry, v. 40, p. 167-173

Fujisawa R., Cho T., Sugahara K., Takizawa Y., Horikawaa Y., Shiomi T., Hironaga M., 1997, The corrosion behaviour of iron and aluminium under waste disposal conditions*, Scientific Basis for Nuclear Waste Management XX, MRS Symp. Proc.* vol. 465, , p. 675

Fujita, N., Matsuura, C., and Saigo, K., 2000, Irradiation-enhanced corrosion of carbon steel in high temperature water -- in view of a cell formation induced by [gamma]-rays*: Radiation Physics and Chemistry*, v. 58, p. 139-147

Fujita, N, 2001, Radiation-induced preferential dissolution of specific planes of carbon steel in high-temperature water: *Radiation Physics and Chemistry,* v. 60, p. 53-60

Fujiwara A., Yasutomi I., Fukudome K., Tateishi T., Fujiwara K., 2001, Influence of Oxygen Concentration and Alkalinity on the Hydrogen Gas Generation by Corrosion of Carbon Steel, *Mat. Res. Soc. Symp*. Vol. 663, MRS 2001, p. 497, Sci Basis XXIV, Sydney

Gdowski G.E., Estill J.C., (1996) The effect of water vapor on the corrosion of carbon steel at 65 oC, Mat. Res. Soc. Symp. Proc. Vol. 412, , MRS. p . 533 – 538

Grauer R., Knecht B., Kreis P., Simpson J.P., 1991, Hydrogen evolution from corrosion of iron and steel in intermediate level waste repositories, *Mat. Res. Soc. Symp. Proc.* Vol.212, MRS, Sci. Basis XIV, Boston, str.295

Hara K., Ishikawa H., Honda A., Sasaki N., 1992, Influence of Dissolved Oxygen on the Generation Rate of Hydrogen Gas with Corrosion of Carbon Steel, *Proceeding of Workshop Gas Generation and Release*, OECD Paris, p. 120

Honda A., Teshima T., Tsurudome K., Ishikawa H., Yusa Y., Sasaki N., 1991, Effect of compacted bentonite on the corrosion behaviour of carbon steel as geological isolation overpack*, Mat. Res. Soc. Symp. Proc.* Vol.212, MRS, Sci. Basis XIV, Boston, str. 287

Ishigure, K.,Fujita N., Tamura, T., Oshima, K., 1980, Effect of gamma radiation on the release of corrosion products from carbon steel and stainless steel in high temperature water. [PWR; BWR]: *Nucl. Technol*. Vol. 50,2,Pages: 169-177

Jelinek J., Neufeld P. , 1982, Kinetics of Hydrogen Formation from Mild Steel in Water under Anaerobic Conditions, *Corrosion*, Vol. 38, No.2, February

Joseph, J.M., Seon, C. B., Yakabuskie, P. C., Wren, J., 2008, A combined experimental and model analysis on the effect of pH and O2(aq) on [gamma]-radiolytically produced H2 and H2O2: Radiation Physics and Chemistry, v. 77, p. 1009-1020.

Lapuerta, S., Moncoffre, N., Millard-Pinard, N., Mendes, E., Corbel, C., and Crusset, D., 2005, use of ion beam analysis techniques to characterise iron corrosion under water radiolysis Nuclear Instruments and Methods in Physics Research Section B: Beam Interactions with Materials and Atoms, v. 240.

Lapuerta, S.M.-P., N; Moncoffre, N.;Bererd, N.; Jaffrezic, H.; Brunel, G.;Crusset, D.;Mennecart, Th, 2007, Origin of the hydrogen involved in iron corrosion under irradiation: Surface and Coatings Technology, v. 201, p. 8197-8201.

Lapuerta, S., Moncoffre N., Bererd, N., Jaffrezic, H., Millard-Pinard, N, Crusset, D., 2006, Ion beam analysis of the effect of O2 and H2O on the oxidation of iron under irradiation: *Nuclear Instruments and Methods in Physics Research Section B: Beam Interactions with Materials and Atoms*, v. 249, p. 470-473.

Lillard, R.S.P., D. L.;Butt, D. P., 2000, The corrosion of materials in water irradiated by 800 MeV protons: *Journal of nuclear materials,* v. 278, p. 277-289.

Manaka, Mitsuo Kawasaki, Manabu Honda, Akira, 2000 Measurements of the effective diffusion coefficient of dissolved oxygen and oxidation rate of pyrite by dissolved oxygen in compacted sodium bentonite, *Nuclear Technology*, v. 130(2), p. 206-217

Marsh G.P., Taylor K.J., Sharland S.M., Tasker P.W., 1987, An approach for evaluation the general and localised corrosion of carbon-steel containers for nuclear waste disposal, in *Scientific Basis for Nuclear Waste Management X, Mat. Res. Soc. Sym Proc*. Vol. 84 str. 227

Marsh, G.P., and Taylor, K.J., 1988, An assessment of carbon steel containers for radioactive waste disposal: *Corrosion Science,* v. 28, p. 289-320

Matsuda F., Wada R., Fujiwara K., Fujiwara A.,1995, An evaluation of hydrogen evolution from corrosion of carbon steel in low/intermediate level waste repositories, MRS, Symp-Proc. Vol. 353, Eds. Murakami T, Ewing R.C. *Scientific Basis for Nuclear Waste Management XVIII*, Kyoto, str.719

Nielsen, F.L., Karin;Jonsson, Mats, 2008, Simulations of H2O2 concentration profiles in the water surrounding spent nuclear fuel: *Journal of nuclear materials*, v. 372, p. 32-35.

Pastina, B., 1997, Etude sur la radiolyse de l'eau en relation avec le circuit primaire de refroidissement des réacteurs nucléaires à eau sous pression: Orsay, Partis XI

Pastina, B.I., J.; Hickel, B., 1999, The influence of water chemistry on the radiolysis of the primary coolant water in pressurized water reactors: *Journal of nuclear materials*, v. 264, p. 309-318.

Platts N., Blackwood D.J., Naish C.C., 1994, Anaerobic oxidation of carbon steel in granitic groundwaters: A review of the relevant literature, *SKB Technical Report 94-01*,

Puigdomenech I., Ambrosi J-P., Eisenlohr L., Lartique J-E., Banwart S.A., Bateman K., Milodowski A.E., West J.M., Griffault L., Gustafsson E., Hama K., Yoshida H., Kotelnikova S., Pedersen K., Michaud, Trotignon L., Rivas Perez J., Tullborg E-L. , 2001, O2 depletion in granitic media The Rex project, *Technical Report SKB TR-01-05*

Puigdomenech I., Taxen C., 2000, Thermodynamic data for copper: Implications for the corrosion of copper under repository conditions, *Technical Report SKB TR-00-13*,

Puigdomenech I., Trotignon L., Kotelnikova S., Pedersen K., Griffault L., Michaud V., Lartigue J--E., Hama K., Yoshida H., West J.M., Bateman K., Milodowski A.E., Banwari S.A., Rivas Perez J., Tullborg E.-L.,2000, O2 consumption in a granitic environment, *Mat. Res. Symp. Proc. Vol. 608, MRS, Sci Basis XXIII*, Boston, p. 179

Rasmussen, O.L.B.E., 1984, Chemsimul - a program package for numerical simulation of chemical reaction systems. , *in* Rissô National Laboratory, D., ed., *Technical Report Risö-R-395 (ENG*)

Ross, A.B., Mallard W.G., Helman W.P., Buxton G.V., Huie P. E., Neta P.,, 1994, Solution Kinetics Database - Version2.0 NIST Gaitherburg USA, *in* NDRL-NIST, ed.

Ross, A.B., Neta P., 1979, rate constants for reactions of inorganic radicals in aqueous solutions, *NSRDS - NBS 65.* 58p.

Schenk R.,1988, Untersuchungen uber die wasserstoffbildung durg eisencorrosion unter endlagerbedingungen, *NAGRA Technisher bericht 86-24*,

Simpson J.P.,1984, Experiments on Container Materials for Swiss High-Level Waste Disposal Projects Part II, *NAGRA Technical report 84-01*

Simpson J.P., Schenk R., 1987, Hydrogen evolution from corrosion of pure copper, *Corrosion Science,* Vol. 27, pp. 1365-1370

Simpson J.P., Schenk R., Knecht B., 1985, Corrosion rate of unalloyed steels and cast irons in reducing granitic groundwaters and chloride solutions*, Sci Basis for Nuclear Waste Management X, Mat. Res. Soc. Sym Proc.* Vol. 50, Ed- L.O. Werme, p. 429

Smart N.R., Blackwood D.J., Werme L., 2001, The anaerobic corrosion of carbon steel and cast iron in artificial groundwaters, SKB Technical Report TR 01-22

Smart N.R., Bond A.E., Crossley J.A.A., Lovegrove P.C., Werme L., 2001, Mechanical properties of Oxides Formed by Anaerobic Corrosion of Steel, *Mat. Res. Soc. Symp. Vol. 663, MRS*, p. 477, Sci Basis XXIV, Sydney 2000

Smart N.R., Rance A.P., Werme L.O., 2004, Anaerobic corrosion of steel in bentonite, Mat. Res..Soc.Symp.Prpc. Vo.807, 2004, Materials Research Society

Smart N.R., Rance A.P., Fennell P, Werme L., 2002, Expansion due to anaerobic corrosion of steel and cast iron: experimental and natural analogue studies, In: Prediction of long term corrosion behaviour in nuclear waste systems. *Proccedings of an int. Workshop, Cadarache, France* , pp. 280-294

Smart, N.R.R., Rance A. P.;Werme, L. O., 2008, The effect of radiation on the anaerobic corrosion of steel: *Journal of nuclear materials*, v. 379, p. 97-104.

Spotheim-Maurizot, M., Mostafavi, M., Douki, Y., and Belloni, J., 2008, *Radiation Chemistry, l'actualité chimique,* EDP Sciences.

VOKÁL A., BRŮHA P., DOBREV D., POLÍVKA P., SILBER R. 2007. A study of anaerobic corrosion of carbon steel, Deliverable 2.3.8, NF-PRO project, August 2007.

Wasselin-Trupin, V., 2000, Processus primaires en chimie sous rayonnement. Influence du Transfert d'Energie Linéique sur la radiolyse de l'eau. : Orsay, Paris XI.

Wiborgh M., Hoglund L.O., Pers K., 1986, Gas formation in a L/ILW Repository and gas transport in the host rock, NAGRA Tech. Report 85-17

Xia X., Idemitsu K., Arima T., Inagaki Y., Ishidera T., Kurosawa S., Iijima K., Sato H., 2005, Corrosion of carbon steel in compacted bentonite and its effect on neptunium diffusion under reducing condition, *Applied Clay Science* 28, 89-100

Xu, T., Senger, R., and Finsterle, S., 2008, Corrosion-induced gas generation in a nuclear waste repository: Reactive geochemistry and multiphase flow effects: *Applied Geochemistry,* v. 23, p. 3423-3433.

Yakabuskie, P.A.J., Jiju M.;Clara Wren, J., 2010, The effect of interfacial mass transfer on steady-state water radiolysis: *Radiation Physics and Chemistry*, v. In Press, Accepted Manuscript.

Zhang, X., Xu, W., Shoesmith, D.W., and Wren, J.C., 2007, Kinetics of H2O2 reaction with oxide films on carbon steel: *Corrosion Science,* v. 49, p. 4553-4567.

Appendix 1: Composition of clay pore waters for 3 different clay dry densities

Dry density (kg/cm3)	1300	1600	1900
Porosity	0.122	0.044	0.019
Log PCO_2	- 3.42	-3.47	-3.65
Na (M)	0.183	0.207	0.254
K (M)	0.0027	0.0031	0.0037
Mg (M)	0.01	0.012	0.015
Ca (M)	0.0092	0.0098	0.012
Sr (M)	8.1 E-5	8.6 E-5	1.1 E-4
Cl (M)	0.0181	0.0618	0.17
SO_4 (M)	0.102	0.095	0.071
C_{inorg} (M)	8.9 E-4	8 E-4	5.5 E-4
F (M)	2.2 E-4	2.2 E-4	1.9 E-4
Si (M)	1.8 E-4	1.8 E-4	1.8 E-4

NB: Compositions given by NRI

Appendix 2: Example of input file for CHEMSIMUL

$chemical reactions * équilibres acide base *H20 !pke=15.75 !molecule d'eau=55.5 RE1: H2O+H2O=OH[-]+H3O[+]; A=2.36e-5 RE2: OH[-]+H3O[+]=H2O+H2O; A=1.3e11... * reactions with e-aq RE15: E[-]+E[-]=H2+OH[-]+OH[-]; A=5.5E9 RE16: E[-]+H=H2+OH[-]; A=2.54E10 *reactions with radical H RE25: H + O[-] = OH[-] ; A=1E10.. * reactions with radical OH RE33: OH+H2=H2O+H; A=6e7 RE34: OH + OH = H2O2 ; A=5.5E9..... * reactions with radical HO2 RE40: HO2+O2[-]=HO2[-]+O2; A=9.7e7 RE41: HO2+HO2=H2O2+O2; A=8.3e5 * reactions with radical O[-] RE42: O[-] + H2 = H + OH[-] ; A=1.E8.. * reactions with radical O3[-] RE50: O3[-] = O2 + O[-] ; A=2.6E3.... * reactions with carbonates RE63: HCO3[-]+OH=CO3[-]+H20; A=8.5e6... * reactions with solution species (sulphate, nitrate..)	Solution composition $concentrations déduites de Jchess eau-oxygene con(H3O[+])=0 con(HCO3[-])=2.2e-6 con(H2CO3)=1.0735e-5 con(H20)=55.5e0 con(OH[-])=0 con(O2)=2.52e-4 con(CO3[--])=4.71e-11 $integration eps=1.0e-5 *fststp=5.0e-7 *hmax=5.0e-3 tend=1.296e6 *jt= $output control *derivative(O2) dig=3 mathinfo diffeq linele=80 prints=110 radprs=110